

# LISA Long-arm Interferometry

**James Ira Thorpe**

NASA/GSFC, Greenbelt, MD 20771, USA

E-mail: [james.i.thorpe@nasa.gov](mailto:james.i.thorpe@nasa.gov)

## **Abstract.**

The Laser Interferometer Space Antenna (LISA) will observe gravitational radiation in the milliHertz band by measuring picometer-level fluctuations in the distance between drag-free proof masses over baselines of approximately  $5 \times 10^9$  m. The measurement over each baseline will be divided into three parts: two 'short-arm' measurements between the proof masses and a fiducial point on their respective spacecraft, and a 'long-arm' measurement between fiducial points on separate spacecraft. This work focuses on the technical challenges associated with these long-arm measurements and the techniques that have been developed to overcome them.

PACS numbers: 95.55.Ym, 04.80.Nn, 07.60.Ly

## **1. Introduction**

Gravitational waves from distant astrophysical sources can be detected by monitoring the deviation between two or more inertial test particles separated over a long baseline. The Laser Interferometer Space Antenna [1] (LISA) is a realization of such a detector in the  $10^{-4} \text{ Hz} \leq f \leq 10^{-1} \text{ Hz}$  frequency band, a regime rich in astrophysical sources [2]. The instrument consists of three separate sciencecraft (SC) in a triangular formation approximately 5 Gm on a side. By monitoring the distance between reference points on separate SC with a precision of  $\sim 10^{-11}$  m, gravitational wave signals with strains on the order of  $\sim 10^{-21}$  can be observed.

The test particles for the LISA measurement are the gravitational reference sensors (GRSs), each consisting of a 4 kg cube of Au-Pt alloy known as a "proof-mass" that floats freely inside an electrode housing. A control system maintains the gap between the proof mass and the housing by actuating thrusters on the SC, a scheme known as drag-free control.

Each SC contains two GRS units, one oriented towards each of the other SC, as shown in 1. The goal of the interferometric measurement system (IMS) is to monitor the distance fluctuations along each of the six one-way links between the proof-masses on separate SC. For convenience, each one-way measurement is broken into three sub-measurements: two short-arm measurements of the distance between each proof-mass

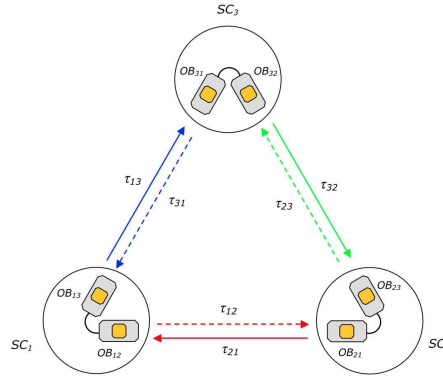


**Figure 1.** The LISA constellation consists of three sciencecraft (SC), each containing two optical benches (OBs). The long-arm measurement consists of measuring displacements along each of the six one-way links, characterized by  $\tau_{ij}$ , the light travel time from  $SC_i$  to  $SC_j$ .

and a reference point on its host SC and a long-arm measurement between reference points on the two separate SC.

This work focuses on the long-arm measurement and relevant aspects of the subsystems involved in making it. Section 2 describes the subsystems that are involved in the long-arm interferometry while section 3 describes how the problem of laser phase noise is addressed. As with other recent review articles [3, 4], the intent is to give an overview of work done by the community of researchers contributing to LISA interferometry, of which the author is but one member.

## 2. Relevant Subsystems

There are several subsystems involved in making the long-arm measurement. In this section, an overview of these subsystems is presented with an emphasis on their role in long-arm interferometry. The subsystems considered are the laser subsystem, the telescope, the optical bench, the pointing mechanisms, and the phase measurement subsystem. It is worth noting that the subsystems discussed here are the ones with the greatest difference between LISA and its technology demonstrator mission, LISA Pathfinder [5, 6] (LPF), a single-SC mission which does not include a long-baseline measurement.

### 2.1. Laser subsystem

The laser subsystem provides the light source for the interferometric measurements. The Nd:YAG laser must deliver a nominal optical power of  $\sim 1$  W at  $1.064 \mu\text{m}$  to the transmitting telescope. The center frequency of the laser must be tunable, both to enable heterodyning between multiple laser sources and to allow the laser frequency/phase to be actively controlled to suppress the intrinsic noise of the laser. A final requirement

for the laser system is the ability to phase modulate the laser at high frequency (several GHz), a capability that is used for the clock noise correction discussed in section 2.5.

The current baseline design for the LISA laser is a master-oscillator power-amplified (MOPA) architecture. The master oscillator, in the form of a non-planar ring oscillator (NPRO) such as the one that will fly on LPF or a fiber laser[7], produces a low-power beam which can be frequency tuned. Light from the master laser is modulated in a waveguide phase modulator and used to seed a fiber amplifier which produces the final output power. This design requires that neither the phase modulator nor power amplifier introduce phase noise at the  $\sim 1 \mu\text{cycle}$  level. Tests of both components are underway and preliminary results indicate that this architecture can meet the requirements [8].

## 2.2. Telescope

The function of the telescope subsystem is to exchange beams between optical benches on separate SC. The primary concern is the amount of power which can be collected by the receiving SC, as this sets the shot noise limit for the displacement measurement. Assuming an end-of-life transmitted power of 0.5 W, the received power will be as low as 100 pW, corresponding to a shot noise limit on displacement of  $\sim 10^{-11} \text{ m}/\sqrt{\text{Hz}}$ [4]. All other IMS noise sources are designed to be below this shot noise limit.

A second concern for the telescope is its mechanical stability, which directly enters the long-baseline measurement. To keep mechanical fluctuations of the telescope below shot noise, the pathlength through the telescope must be stable to  $\sim 1 \text{ pm}/\sqrt{\text{Hz}}$ . If this level of stability cannot be met, an alternative is to measure pathlength fluctuations in the telescope with an auxiliary interferometer and correct for them in post-processing, an arrangement known as an optical truss.

Other concerns for the telescope are the quality of the wavefront delivered to the far SC and the generation of scattered light. Deviations from an ideally spherical wavefront at the receiving SC will cause angular jitter in the transmitting SC to produce a phase shift in the received beam that would be interpreted as a displacement. Light from the transmitting SC may scatter off of the telescope and interfere with the received light, generating an additional heterodyne signal with a phase that is dependent on the stability of the scattering path.

## 2.3. Optical Bench

The function of the optical bench is to interfere the various beams needed to make the displacement measurements. Figure 2 shows a schematic (not a realistic layout) of the bench, with three beams entering the bench. The local beam enters via an optical fiber from the laser subsystem, a beam from the adjacent bench enters via the “back-link” fiber that connects the two benches on each SC, and a beam from the far SC enters via the telescope. The local laser is also transmitted to the far SC via the telescope.

These three beams are used to make three heterodyne interferences. The reference measurement ( $R$ ), combines the local beam with the adjacent beam to measure the

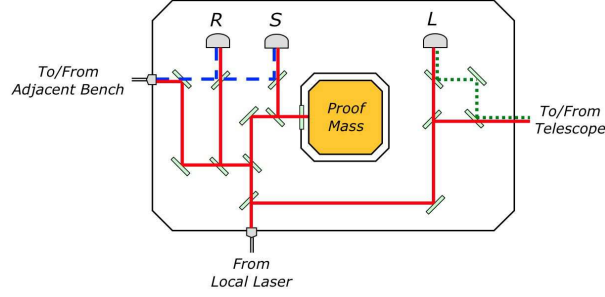


**Figure 2.** Schematic of the LISA optical bench showing three primary interferometric measurements (reference,  $R_{ij}$ , short-arm,  $S_{ij}$ , and long-arm,  $L_{ij}$ ) made using the three beams: from the local laser (solid), from the adjacent bench via the inter-bench fiber (dashed), and from the far SC via the telescope (dotted).

relative phase noise of the two lasers as well as the phase noise in the back-link fiber. The short-arm measurement ( $S$ ) is identical to the reference measurement except that the local beam is reflected off of the proof mass, adding the projected motion of the SC to the measurement. The long-arm measurement ( $L$ ) combines the local beam with the received beam, measuring laser phase noise, motion of both SC, shot noise, and gravitational wave strain. In each of these signals, the heterodyne phase is dominated by the intrinsic phase noise of the interfering beams. The key to LISA interferometry is to measure these signals with high fidelity and then combine them in ways that cancel laser phase noise and other obscuring terms in order to extract the desired quantities.

As with the telescope, the pathlength stability of the optical bench is also critical. The LISA optical bench will be constructed using a technique known as hydroxide-catalysis bonding that has been applied to the LPF optical bench[9, 10]. In this technique, the individual optics are bonded to an ultra-stable glass substrate, yielding a bench with a stability approximately equivalent to that of a monolithic structure.

#### 2.4. Constellation Design and Pointing Mechanisms

The LISA constellation is not actively maintained through station-keeping; each SC is inserted into the appropriate orbit and the constellation geometry evolves along with those orbits. Perturbations from the planets and other bodies cause the orbits to oscillate with an annual period as well as experience secular degradation. Orbits are designed using optimization techniques [11] that seek to constrain some property of the constellation. For example, the orbits in Figure 3 minimize the relative line-of-sight velocities and resulting Doppler shifts in the long-arm heterodyne signals.

The  $\sim 1^\circ$  variations in the interior angle of the LISA constellation are larger than the field of view of the telescope and hence require a mechanism to maintain pointing to both far SC simultaneously. The optical assembly tracking mechanism (OATM) provides this function by pivoting the payload assembly (GRS, optical bench, & telescope) to track one of the far SC while the other one is tracked by adjusting the attitude of

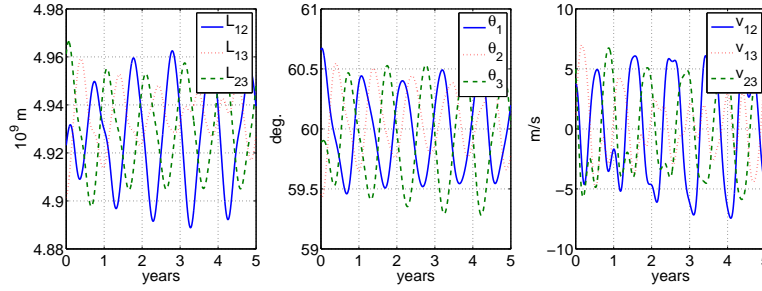


**Figure 3.** Arm-lengths, interior angles, and line-of-sight velocities for one realization of the LISA constellation. This particular realization is designed to minimize the line-of-sight velocities.

the SC. The closed-loop pointing error of the OATM must have a spectral density less than  $\sim 1 \text{ nrad}/\sqrt{\text{Hz}}$  in the LISA band. Achieving this stability and accuracy over a  $1^\circ$  dynamic range requires a multi-stage mechanism or an actuator with high accuracy and large dynamic range, such as a piezo inchworm.

An additional mechanism is needed to compensate for the relative motion between the SC. Due to the light travel time between the SC ( $\tau_{ij} \sim 17 \text{ s}$ ), it is necessary to point the transmitted beam ahead of the position of the received beam. This introduces an angle between the transmitted and received beams on the order of  $\Delta v/c$ , where  $\Delta v$  is the relative velocity between the SC, that must be corrected prior to interfering the beams. For the orbital solution in Figure 3, the angle has a component in the constellation plane with a nominal value of  $\sim 1.6 \mu\text{rad}$  and variations of  $\sim 60 \text{ nrad}$  as well as a component normal to the constellation plane that is approximately a mean-zero sinusoid with an amplitude of  $\sim 3 \mu\text{rad}$ . A mechanism known as the point-ahead actuator<sup>‡</sup> (PAA) corrects for these angles, maintaining alignment between the local and received beam. Unlike the OATM, the PAA is in the interferometric path and consequently must keep any added displacement noise below the  $\sim 1 \text{ pm}/\sqrt{\text{Hz}}$  level.

### 2.5. Phase Measurement Subsystem

The function of the phase measurement subsystem (PMS) is to measure the phase of the heterodyne signals on the six optical benches with sufficient fidelity that they can be combined to measure desired quantities such as SC motion and GW signals. The primary challenge for the PMS is one of dynamic range: the laser phase noise has a spectral density in excess of  $1 = 1 \text{ MHz}/\sqrt{\text{Hz}}$  in the LISA band whereas the desired noise floor for detecting gravitational wave signals is on the order of  $\sim 1 \mu\text{cycle}/\sqrt{\text{Hz}}$ . An additional complication in the  $L$  measurement is the variation of the heterodyne frequency caused by the time-varying Doppler between the SC (see section 2.4).

The PMS can be divided into an analog chain, which converts the optical beat note

<sup>‡</sup> If the actuator is implemented on the received beam, it is sometimes referred to as a look-behind actuator.

into a digital signal, and a digital processor, which extracts the phase of that signal. The analog chain consists of the photoreceiver, amplifiers, and analog-to-digital converters. Each beat note is measured using a quadrant detector, which allows the angle between the interfering beams to be measured by differencing the measured phase from different quadrants. The digital portion of the PMS consists of a digital oscillator that is phase-locked to the heterodyne signal. The phase of the heterodyne signal is extracted by measuring the frequency of the phase-locked oscillator as well as the phase error in the loop. Implementations of the PLL-type PMS [12, 13] have demonstrated the ability to measure LISA-like signals with a dynamic range of better than  $\sim 10^{14}$  in the LISA band, more than sufficient for LISA requirements.

The phase measurements made on each SC will be contaminated by phase noise of the ultra-stable oscillator (USO) used provide the time reference on-board the SC. Ordinarily, the USO phase noise is not a concern as it is common to all measurements made on the SC. In LISA, however, measurements from multiple SC are combined, each with their own independent USO noise. To address this issue, the relative phase noise of each pair of USOs is measured by transmitting a phase modulation tone along each of the inter-SC links[14]. Recording the phase of this tone allows the relative USO clock noise to be removed in post-processing.

### 3. Mitigation of Laser Phase Noise

One of the main challenges for LISA interferometry is mitigation of laser phase noise that couples into the long-arm measurement. In a classic equal-arm Michelson interferometer, the phase noise of the light source does not couple into the displacement measurement because it is common in both interfering beams. In the LISA long-arm interferometer, this is not the case for two reasons: there are two independent light sources and there is significant difference in the arm-length. At a Fourier frequency of 1 mHz, the phase noise spectral density of the free-running LISA lasers is expected to be on the order of  $5 \times 10^9$  cycles/ $\sqrt{\text{Hz}}$ , more than 14 orders of magnitude above the roughly  $10 \mu\text{cycle}$  shot noise limit. The following sections describe how this noise is suppressed in the measurement, allowing LISA to operate at the shot noise limit.

#### 3.1. Time-Delay Interferometry

The goal of Time Delay Interferometry[15, 16] (TDI) is to recover the insensitivity to phase noise that is present in an equal-arm Michelson interferometer. The concept is to combine the phase measurements of the individual links in post processing in order to synthesize an equal-arm interferometer. To do this requires some knowledge of the constellation geometry as well as sufficiently high fidelity in the phase measurements that the cancellation will span the many orders of magnitude needed to reach the target sensitivity.

The ability of TDI to suppress laser frequency noise is limited by a number of

**Table 1.** Phase noise suppression limits for TDI as a function of Fourier frequency  $f$  (Adapted form [17])

Effect	Assumption	Suppression Limit
Arm-length knowledge	ranging error of $\delta x$	$2.4 \times 10^{10} \times (1 \text{ m}/\delta x) \times (1 \text{ mHz}/f)$
Algorithm Errors	velocity-correcting TDI	$2 \times 10^{12} \times (1 \text{ mHz}/f)$
Interpolation Errors	21 s kernel, 3 Hz sampling	$3.2 \times 10^{15} \times (1 \text{ mHz}/f)^2$
Analog Chain Errors	Laboratory measurements	$5 \times 10^{10} \times (1 \text{ mHz}/f)$
PMS noise floor	Laboratory measurements	$10^{14} \times (1 \text{ mHz}/f)^2$
Scattered light	amplitude of $2 \times 10^{-5}$	$1.5 \times 10^{17} \times (1 \text{ mHz}/f)$

effects, the relative importance of which can be expressed using a suppression limit factor defined as the ratio between the input phase noise and the phase noise in the TDI channel. Table 1 lists several limiting effects that have been studied. Arm-length knowledge refers to errors in the assumed values of the light travel times that are used to form the delays in the TDI combinations. Algorithm errors result from limitations in the ability to correct for higher-order terms in the dynamics of the constellation (relative velocity, acceleration, etc. between the SC). Interpolation errors are limits on the accuracy of determining the value of the phase meter signal at a particular time from a series of evenly-spaced points [16]. Analog chain errors refer to effects of dispersion and non-linearity in PMS analog chain. Scattered light errors refer to parasitic heterodyne signals that are generated by stray beams, also known as small vector noise.

The limiting effect for TDI is arm-length knowledge, which can be obtained from a number of sources. In rough order of accuracy they are SC ephemeris models, Doppler tracking of the SC from ground, and active ranging on-board the SC. The baseline ranging system for LISA consists of a pseudo-random noise (PRN) code stream added as a phase-modulation sideband to the clock transfer tones. Additional channels in the PMS measure the phase of the received signal and pass it to the ranging processor, where it is tracked using a delay-locked loop. The current estimate of the ranging error for such a system is  $\delta x \sim 1 \text{ m}$  [18].

The LISA error budget allocates  $2 \text{ pm}/\sqrt{\text{Hz}} \times \sqrt{1 + (3 \text{ mHz}/f)^4}$  to residual laser phase noise, where  $f$  is the Fourier frequency. Assuming ranging-limited TDI, this sets a limit on the maximum allowable laser frequency noise *prior* to TDI,

$$\tilde{\nu}_{pre-TDI}(f) = 282 \text{ Hz}/\sqrt{\text{Hz}} \times \left(\frac{1 \text{ m}}{\delta x}\right) \times \sqrt{1 + \left(\frac{3 \text{ mHz}}{f}\right)^4}. \quad (1)$$

The estimated spectrum for the unstabilized LISA laser is  $30 \text{ MHz}/\sqrt{\text{Hz}} \times (1 \text{ mHz}/f)$ . This leaves a gap of approximately six orders of magnitude between the interferometry requirement and the capability of ranging-limited TDI with 1 m arm length knowledge. Consequently the LISA lasers must be actively stabilized.

### 3.2. Constellation Phase Locking

Active frequency stabilization of the LISA lasers is simplified through the use of phase-lock loops (PLLs). One SC is designated as the master SC and one of its lasers is designated as the master laser. All other lasers in the constellation are phase locked to the master laser which is then stabilized to a frequency reference. An advantage of PLLs is the ability to add an arbitrary frequency offset to the slave lasers. This extra degree of freedom can be used to ensure that all heterodyne frequencies remain in the range of the PMS as the orbital Doppler frequencies change (see section 2.4). It also avoids the problem of having to match the absolute frequencies of multiple independent frequency references to within the PMS bandwidth.

It should be noted that the application of PLLs does not effect the TDI algorithms. The cancellation of laser phase noise in the TDI combinations does not assume any particular correlation between the phase noises from individual lasers, nor is it adversely effected if such correlations exist.

### 3.3. Arm-locking

One option for actively stabilizing the frequency of the master laser is to use the LISA constellation as a frequency reference, a technique referred to as arm-locking. The original proposal for arm-locking, known as single arm-locking[19], showed that the phase of the long-arm heterodyne signal could be used to estimate the laser phase noise. The difficulty with this approach is that this signal is insensitive to phase noise at  $f_n \equiv n/\tau_{RT,j}$  where  $\tau_{RT}$  is the round-trip light travel time in the arm and  $n = 1, 2, 3, \dots$ . These sensor nulls lead to noise enhancement spikes in the closed-loop system at the  $f_n$  frequencies, which populate the LISA measurement band. In addition, the slope of the loop gain for  $f > f_1$  is limited by the phase response of the sensor. Despite these drawbacks, single-arm locking is able to provide significant frequency noise suppression for  $f \neq f_n$  and has been demonstrated in a number of hardware models[20, 21, 22, 23].

Sensitivity to phase noise at  $f = f_n$  can be recovered by utilizing the adjacent LISA arm [24], which generally has a different value for  $\tau_{RT}$  and hence a different set of  $f_n$ . With two arms to provide the information, all frequencies are covered other than those that are multiples of the inverse difference in the round trip times,  $f'_n \equiv n/\Delta\tau_{RT}$  where  $\Delta\tau_{RT} \equiv |\tau_{RT,1} - \tau_{RT,2}|$ . At these frequencies, the null points of the two individual arms overlap and the same issues of instability arise. However, because  $\Delta\tau_{RT}/\tau_{RT} \sim 0.01$ , the  $f'_n$  frequencies lie above the LISA measurement band.

There is some design freedom in determining how best to combine the information from the two long-arm measurements. The goal is to generate a sensor with a flat, broadband response to laser phase noise and minimal coupling of phase noise from other sources, a problem that can be approached using optimization techniques[25] or traditional control design methods. The current baseline arm-locking sensor is the *modified dual arm-locking* sensor, described by McKenzie, et al. [26].

Figure 4 shows the performance of a system based on this sensor and a



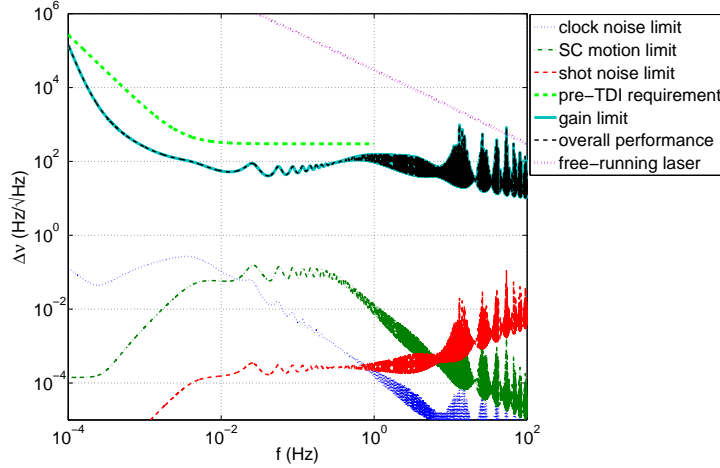


**Figure 4.** Performance of a modified dual arm locking system [26] assuming free-running lasers and an arm-length mismatch of  $\Delta\tau_{RT} = 0.037$  s, the minimum value for the orbits in Figure 3.

complimentary controller design assuming a free-running frequency noise of  $30 \text{ kHz}/\sqrt{\text{Hz}}$  for the master laser. The curves are plotted assuming  $\Delta\tau_{RT} = 0.037$  s, the minimum value for the orbits in Figure 3 assuming that the master SC can be switched at any time to maximize  $\Delta\tau_{RT}$ . The curve labeled 'pre-TDI requirement' is the maximum allowable frequency noise at the input to TDI, assuming 1 m ranging accuracy (see section 3.1).

If a situation were to arise where one of the long-baseline links was not functional, it would not be possible to switch the master SC and  $\Delta\tau_{RT}$  would occasionally reach zero. McKenzie estimates that this system would still meet LISA requirements except during periods of minimum  $\Delta\tau_{RT}$  lasting approximately 30 min and occurring twice per year.

In addition to the gain and noise limitations to arm-locking described above, there is an important limitation associated with the dynamic range of the laser frequency. The PMS measures the phase of the long-arm heterodyne signal relative to a reference signal at the expected heterodyne frequency. Finite knowledge of the inter-SC Doppler shift introduces a mismatch in these frequencies, which is manifested in the PMS output by a ramping phase term.. As the arm-locking controller attempts to correct for this term, it pulls the laser frequency, risking bringing the master laser, or one of the other phase-locked lasers, into an unstable operating regime. The problem of laser pulling can be mitigated by improving estimates of the Doppler frequency and AC-coupling the arm-locking controller to reduce the effects of Doppler errors.

### 3.4. Local Stabilization

Another option is to stabilize the master laser to a frequency reference on-board the SC. This is the approach taken by LISA Pathfinder, which uses a Mach-Zender (MZ) interferometer with a deliberate pathlength difference to measure and correct

for frequency fluctuations[27]. The performance of such a system is limited by the pathlength stability of the MZ, which is integrated into the optical bench, and the noise floor of the PMS. The expected performance is approximately  $1 \text{ kHz}/\sqrt{\text{Hz}} \times \sqrt{1 + (3 \text{ mHz}/f)^4}$ . While this performance is not sufficient to reach the pre-TDI requirement, the MZ can serve as a pre-stabilization stage for arm-locking, reducing the requirements on arm-locking and increasing overall system margin.

The best-performing standard frequency references in the LISA band are high-Finesse optical cavities[28]. Mueller, et al. [29] demonstrated performance of better than  $30 \text{ Hz}/\sqrt{\text{Hz}} \times \sqrt{1 + (3 \text{ mHz}/f)^4}$  in the LISA band, capable of meeting the pre-TDI requirement even if the ranging accuracy is relaxed to 10 m.

In order to use an optical cavity as a pre-stabilization stage for arm-locking, it is necessary to provide a way to adjust the center frequency of the laser while still maintaining the stability provided by the cavity. The preferred method for doing this is offset sideband locking[30], which modifies the standard Pound-Drever-Hall readout scheme to allow the laser frequency to have an adjustable offset from the cavity resonance. This avoids the problems with corrupting the intrinsic stability of the reference that arise when an adjustable element such as a piezo-electric actuator is added to the cavity itself [31].

### 3.5. Reference Designs

In this section we consider four reference designs for laser phase noise mitigation that meet LISA requirements. These designs were proposed in a whitepaper [17] prepared by the LISA Frequency Control Working Group, an ad-hoc assembly of frequency control researchers from government agencies, universities, and industry who are actively working on LISA.

TDI with 1 m ranging accuracy is common to all designs, setting the maximum pre-TDI frequency noise limit as  $282 \text{ Hz}/\sqrt{\text{Hz}} \times \sqrt{1 + (3 \text{ mHz}/f)^4}$ . All lasers are assumed to be phase locked to a single master laser, as described in section 3.2. In designs where arm-locking is included, it is implemented using the modified dual arm-locking as described by McKenzie, et al.[26]. Arm-locking performance is computed assuming a minimum round-trip difference of  $\Delta\tau_{RT} = 0.037 \text{ s}$ , corresponding to the minimum difference in the orbits described in Figure 3, assuming all inter-SC links are available.

Figure 5 illustrates the noise performance of the four reference designs, which are described below.

- Fixed Cavity (thin dot-dashed line): Master laser locked to a fixed Fabry-Perot cavity using standard techniques.
- Arm-locking only (thin solid line): Master laser locked using modified dual arm locking.
- Arm-locking with MZ pre-stabilization (thin dotted line): Master laser pre-stabilized to MZ interferometer with offset. Additional stabilization provided by modified dual arm-locking.

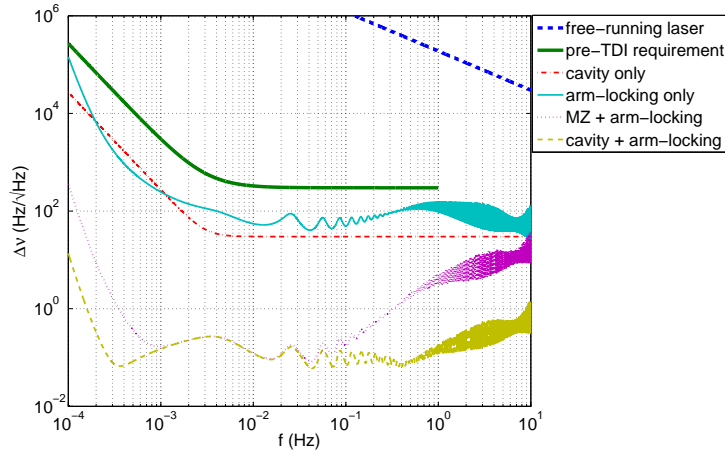


**Figure 5.** Possible options for laser phase noise suppression in LISA. See text for details.

- Arm-locking with cavity pre-stabilization (thin dashed line): Master laser pre-stabilized to fixed Fabry-Perot cavity with an offset using sideband locking technique. Additional stabilization provided by modified dual arm locking.

For each design, the noise performance lies below the pre-TDI limit (thick solid line). The selection of a particular design for LISA will be based on criteria other than noise performance such as complexity, cost, easy of ground testing and integration, etc.

#### 4. Summary

The measurement of  $10^{-11}$  m displacements over  $5 \times 10^9$  m baselines is one of the technological capabilities that will allow LISA to measure gravitational waves. Achieving this capability will require overcoming a number of challenges. Thanks to the work of a large number of researchers over many years, a design for the LISA long-arm interferometer that meets these challenges has been developed.

#### Acknowledgments

In addition to recognizing the contributions of the community as a whole, I would like to thank Kirk McKenzie for providing the tools needed to compute arm-locking performance, Steve Hughes for providing LISA orbital data, and Bob Spero for helpful discussions on TDI limitations.

Copyright (c) 2010 United States Government as represented by the Administrator of the National Aeronautics and Space Administration. No copyright is claimed in the United States under Title 17, U.S. Code. All other rights reserved.

## References

- [1] P. Bender, K. Danzmann, and the LISA Study Team. Laser interferometer space antenna for the detection of gravitational waves, pre-phase a report. Technical Report MPQ233, Max-Planck-Institut für Quantenoptik, Garching, 1998.
- [2] S.A. Hughes. A brief survey of LISA sources and science. In S.M. Merkowitz and J.C. Livas, editors, *Laser Interferometer Space Antenna: 6th International LISA Symposium*, volume 873, pages 13–20, 2006.
- [3] D.A. Shaddock. Space-based gravitational wave detection with LISA. *Class. Quant. Grav.*, 25(114012), 2008.
- [4] O. Jennrich. LISA technology and instrumentation. *Class. Quant. Grav.*, 26(153001), 2009.
- [5] P. McNamara, S. Vitale, and K. Danzmann. LISA pathfinder. *Class. Quant. Grav.*, 25(114034), 2008.
- [6] M. Armano and et al. LISA pathfinder: the experiment and the route to LISA. *Class. Quant. Grav.*, 26(094001), 2009.
- [7] K. Numata. Fiber laser development for LISA. *Journal of Physics: Conference Series*, 2010. Submitted for Amaldi 8 Conference Proceedings.
- [8] M. Tröbs, S. Barke, J. Möbius, M. Engelbrecht, D. Kracht, L.d’Arcio, G. Heinzel, and K. Danzmann. Lasers for LISA: overview and phase characteristics. *Journal of Physics: Conference Series*, 154(012016), 2009.
- [9] E. Elliffe and et al. Hydroxide-catalysis bonding for stable optical systems for space. *Class. Quant. Grav.*, 22:S257–67, 2005.
- [10] C. Killow and et al. Construction of the ltp optical bench interferometer. In S.M. Merkowitz and J.C. Livas, editors, *Proceedings of the Sixth International LISA Symposium*, volume 873, pages 297–303, 2006.
- [11] S.P. Hughes. General method for optimal guidance of spacecraft formations. *Journal of Guidance, Control, and Dynamics*, 31(2), 2008.
- [12] D.A. Shaddock, B. Ware, P. Halverson, R.E. Spero, and B. Klipstein. An overview of the LISA phasemeter. In S.M. Merkowitz and J.C. Livas, editors, *Proceedings of the Sixth International LISA Symposium*, volume 873, pages 654–660. AIP Conference Proceedings, 2006.
- [13] I. Bykov, J.J. Esteban Delgado, A.F. Garcia Marin, G. Heinzel, and K. Danzmann. LISA phasemeter development: Advanced prototyping. *Journal of Physics: Conference Series*, 154(012017), 2009.
- [14] W. Klipstein, P.G. Halverson, R. Peters, R. Cruz, and D.A. Shaddock. Clock noise removal in LISA. In S.M. Merkowitz and J.C. Livas, editors, *Laser Interferometer Space Antenna: 6th International LISA Symposium*, volume 873, pages 312–318, 2006.
- [15] M. Tinto and J.W. Armstrong. Cancellation of laser frequency noise in an unequal arm detector of gravitational waves. *Physical Review D*, 59(102003), 1999.
- [16] D.A. Shaddock, B. Ware, R.E. Spero, and M. Vallisneri. Post-process time delay interferometry for LISA. *Physical Review D*, 70(081101(R)), 2004.
- [17] D.A. Shaddock and et al. LISA frequency control white paper. LISA Project technical note LISA-JPL-TN-823, Laser Interferometer Space Antenna, 2009.
- [18] J.J. Esteban Delgado, I. Bykov, A.F. Garcia Marin, G. Heinzel, and K. Danzmann. Optical ranging and data transfer development for LISA. *Journal of Physics: Conference Series*, 154(012025), 2009.
- [19] B.S. Sheard, M.B. Gray, D.E. McClelland, and D.A. Shaddock. Laser frequency stabilization by locking to a LISA arm. *Physics Letters A*, 320(1):9–21, 2003.
- [20] A.F. Garcia Marin, G. Heinzel, R. Schilling, V. Wand, F. Guzman Cervantes, F. Steier, O. Jennrich, A. Wiedner, and K. Danzmann. Laser phase locking to a LISA arm: Experimental approach. *Class. Quant. Grav.*, 22:S235–S242, 2005.
- [21] J.I. Thorpe and G. Mueller. Experimental verification of arm-locking for LISA using electronic

- phase delay. *Physics Letters A*, 342:199–204, 2005.
- [22] V. Wand, Y. Yu, S. Mitryk, D. Sweeney, A. Preston, D. Tanner, G. Mueller, J.I. Thorpe, and J.C. Livas. Implementation of armlocking with a delay of 1 second in the presence of doppler shifts. *Journal of Physics: Conference Series*, 154(012024), 2009.
  - [23] B.S. Sheard, M.B. Gray, D.A. Shaddock, and D.E. McClelland. Laser frequency noise supression by arm locking in LISA: progress towards a bench-top demonstration. *Class. Quant. Grav.*, 22(S221-S226), 2005.
  - [24] A. Sutton and D.A. Shaddock. Laser frequency stabilization by dual arm locking for LISA. *Physical Review D*, 78(082001), 2008.
  - [25] P.G. Maghami, J.I. Thorpe, and J.C. Livas. Arm locking for the laser interferometer space antenna. In *Proceedings of the SPIE Symposium on Advanced Wavefront Control:methods, Devices, and Applications VIII*, volume 7466, pages M1–M11. SPIE, August 2009.
  - [26] Kirk McKenzie, Robert E. Spero, and Daniel A. Shaddock. The performance of arm locking in LISA. submitted, 2009.
  - [27] F. Steier, F. Guzman Cervantes, A.F. Garcia Marin, D. Gerardi, G. Heinzel, and K. Danzmann. The end-to-end testbed of the optical metrology system on-board LISA pathfinder. *Class. Quant. Grav.*, 26(094010), 2009.
  - [28] R.W.P. Drever, J.L. Hall, F.V. Kowalski, J. Hough, G.M. Ford, and A.J. Munley. Laser phase and frequency stabilization using an optical resonator. *Applied Physics B*, 31:97–105, 1983.
  - [29] G. Mueller, P. McNamara, J.I. Thorpe, and J. Camp. Laser frequency stabilization for LISA. Technical Report NASA/TM-2005-212794, NASA, December 2005.
  - [30] J.I. Thorpe, J.C. Livas, and K. Numata. Laser frequency stabilization and control through offset sideband locking to optical cavities. *Optics Express*, 16(20):15980–15990, 2008.
  - [31] L. Conti, M. De Rosa, and F. Marin. High-spectral-purity laser system for the auriga detector optical readout. *JOSA B*, 20(3):462–468, 2003.